Experimental Verification of a Progressive Damage Model for IM7/5260 Laminates Subjected to Tension-Tension Fatigue

TIMOTHY W. COATS
Graduate Research Assistant
Department of Engineering Mechanics
Old Dominion University
Norfolk, VA 23508

CHARLES E. HARRIS*
Head, Mechanics of Materials Branch
Mail Stop 188E
NASA Langley Research Center
Hampton, VA 23681

(Received August 30, 1993)

ABSTRACT: The durability and damage tolerance of laminated composites are critical design considerations for airframe composite structures. Therefore, the ability to model damage initiation and growth and predict the life of laminated composites is necessary to achieve structurally efficient and economical designs. The purpose of this research is to experimentally verify the application of a continuum damage model to predict progressive damage development in a toughened material system. Damage due to monotonic and tension-tension fatigue was documented for IM7/5260 graphite/bismaleimide laminates. Crack density and delamination surface area were used to calculate matrix cracking and delamination internal state variables to predict stiffness loss in unnotched laminates. A damage dependent finite element code predicted the stiffness loss for notched laminates with good agreement to experimental data. It was concluded that the continuum damage model can adequately predict matrix damage progression in notched and unnotched laminates as a function of loading history and laminate stacking sequence.

KEY WORDS: composites, graphite/epoxy, damage, matrix cracks, delamination, internal state variables.

*Author to whom correspondence should be addressed.

Reprinted from *Journal of* COMPOSITE MATERIALS, *Vol. 29, No. 3/1995*

INTRODUCTION

BECAUSE OF THEIR light weight and high specific stiffness, laminated continuous fiber-reinforced composite materials are being used in some primary load bearing components in aircraft structures. However, when subjected to high service loads, environmental attack, impact, or a combination of any or all of the above, laminated composite materials develop damage. As the service load or the time in service increases, damage develops and grows, becoming more severe, and could eventually lead to catastrophic failure.

There are four main types of damage. These are matrix cracking, fiber-matrix interface debonding, delamination, and fiber fracture. Usually, matrix cracking and fiber-matrix interface debonding are the first forms of damage to occur, followed by delamination, and finally fiber fracture resulting in catastrophic failure. While matrix cracking is usually arrested at the fibers or adjacent plies, it will result in a redistribution of load to the surrounding regions. As a result, these surrounding regions contain stress fields which are favorable to the initiation and propagation of additional damage. During the accumulation of subcritical damage, changes in material stiffness and strength results in the load redistribution until the principle load-carrying plies are unable to support the load, in which case, catastrophic failure occurs.

The initiation and propagation of damage is one of the problems in using laminated continuous fiber composite structures. To address durability and damage tolerance requirements, damage must be modelled and methods developed to predict the residual strength and life of composite structures. For example, one of the most complicated structural configurations is that of built-up laminated composite structures connected by mechanical fasteners such as rivets. These laminates with fastener holes develop local damage that cannot be easily treated using stress concentration factors. Another example is the non-visible damage that develops during foreign object impacts and ground handling accidents. Current methods for treating these local damage details are empirical and very conservative. Therefore, an accurate model of the damage initiation and propagation will enhance current analysis and design capabilities thus leading to improvements in structural efficiency.

Many damage progression models are being developed to model damage and predict life. An example of the type of microcrack damage that is currently being studied by damage models is shown by the X-ray radiograph in Figure 1. This damage is both stacking sequence dependent and loading history dependent. An overview of damage resulting from fatigue loading in composites has been presented by Reifsnider [1,2]. Some researchers have tried to model this damage by considering each crack as an internal boundary and the stress or displacement fields are obtained either in closed form or numerically, such as in finite elements. This approach works well as long as there are a relatively small number of cracks. Talug and Reifsnider [3] have obtained finite difference approximate solutions to equilibrium equations to solve for interlaminar stresses in composite laminates. The "damage tolerance/fail safety methodology" developed by O'Brien [4] is an engineering approach to ensuring adequate durability and damage toler-

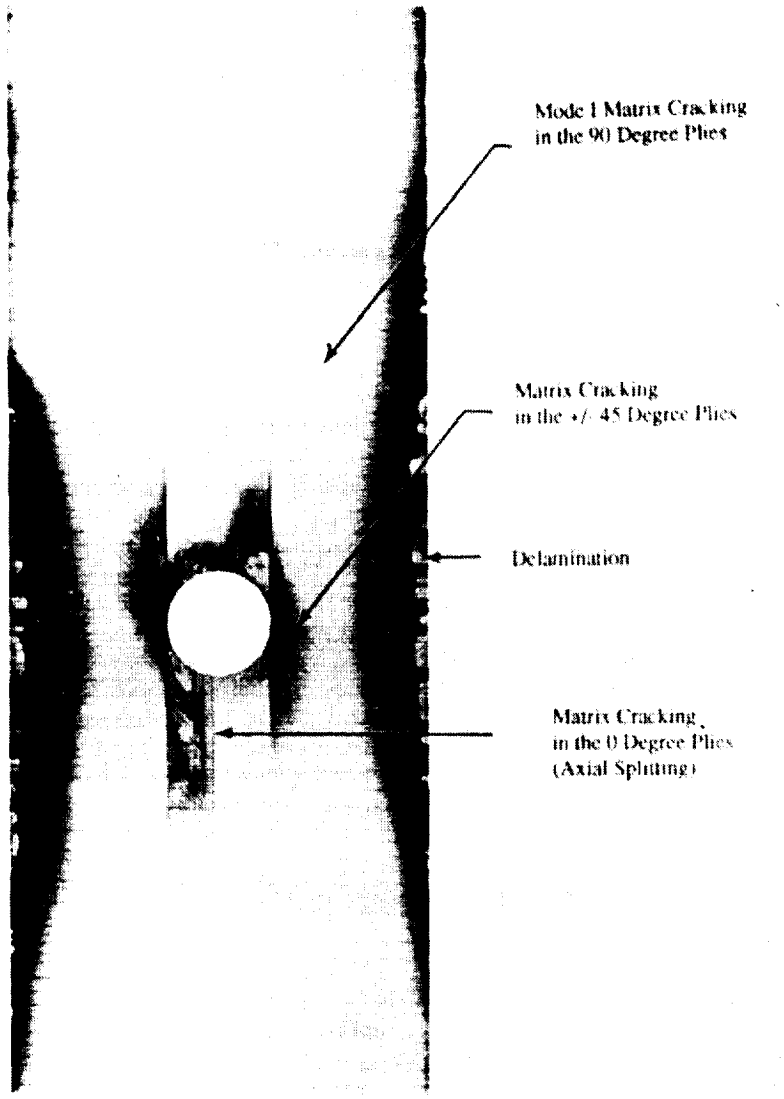

Figure 1. *Tension-tension fatigue damage in a notched* $[0/45/-45/90]_s$ *IM7/5260 laminate.*

ance by treating only delamination onset and the subsequent delamination accumulation through the laminate thickness. Chang [5] developed a progressive damage model for notched composite laminates subjected to monotonic tensile loading. This particular model assesses the damage and predicts the ultimate tensile strength in laminates with arbitrary ply-orientations via an iterative combination of stress analysis and failure analysis. Chamis [6] studied structural characteristics such as natural frequencies and buckling loads and the corresponding mode shapes during progressive fracture of angle-plied polymer matrix composites. This study concluded that the individual nature of the structural change was dependent on laminate configuration, fiber orientation, and the boundary conditions. The model proposed by Talreja [7–9] incorporates internal state variables (ISVs) for matrix cracks and delaminations and exhibits ply stacking sequence dependence. The ISVs are strain-like quantities which represent the damage as volume averaged quantities, i.e., a continuous medium.

The treatment of a damaged volume of material as a continuous medium and the representation of the damage with averaged quantities was first proposed by Kachanov [10] in 1958 and is referred to as continuum damage mechanics. From continuum damage mechanics has evolved the continuum damage model developed by Allen and Harris [11–16]. This damage model utilizes ISVs and is phenomenological; however, it is formulated at the ply and sublaminate level and therefore accounts for the influence of stacking sequence and geometry.

The goal of the research presented in this paper is to apply the Allen and Harris model to a toughened matrix composite system and to experimentally verify the current predictive capability of the model. The IM7/5260 material system was selected for characterization because the 5260 bismaleimide is a candidate elevated temperature polymer for the next generation supersonic transport airplane. Both cross-ply and quasi-isotropic laminates were investigated in unnotched and open-hole specimen configurations. Tension-tension fatigue loading was used to initiate and propagate damage at several different constant amplitude stress levels. No new mathematical models were developed for this study. This investigation was intended to be an interrogation of the suitability of the mechanics framework and the current capabilities of the model to predict damage growth in laminated composites.

THE ALLEN AND HARRIS MODEL

The damage model of Allen and Harris [11–16] was developed to model the behavior of microcrack damage in a brittle epoxy material system by predicting stiffness loss and damage-dependent ply level stresses in a laminate. A summary of the model can be found in the literature [17]. The model, which neglects edge effects, uses internal state variables to represent the local deformation effects of various modes of damage. Loading history dependence is modelled by ISV damage growth laws. The progression of damage is predicted by an iterative and incremental procedure outlined in the flowchart shown in Figure 2. This entire progressive failure analysis scheme has been implemented into the NASA Computational Mechanics Testbed (COMET) [18]. The first block of Figure 2 is

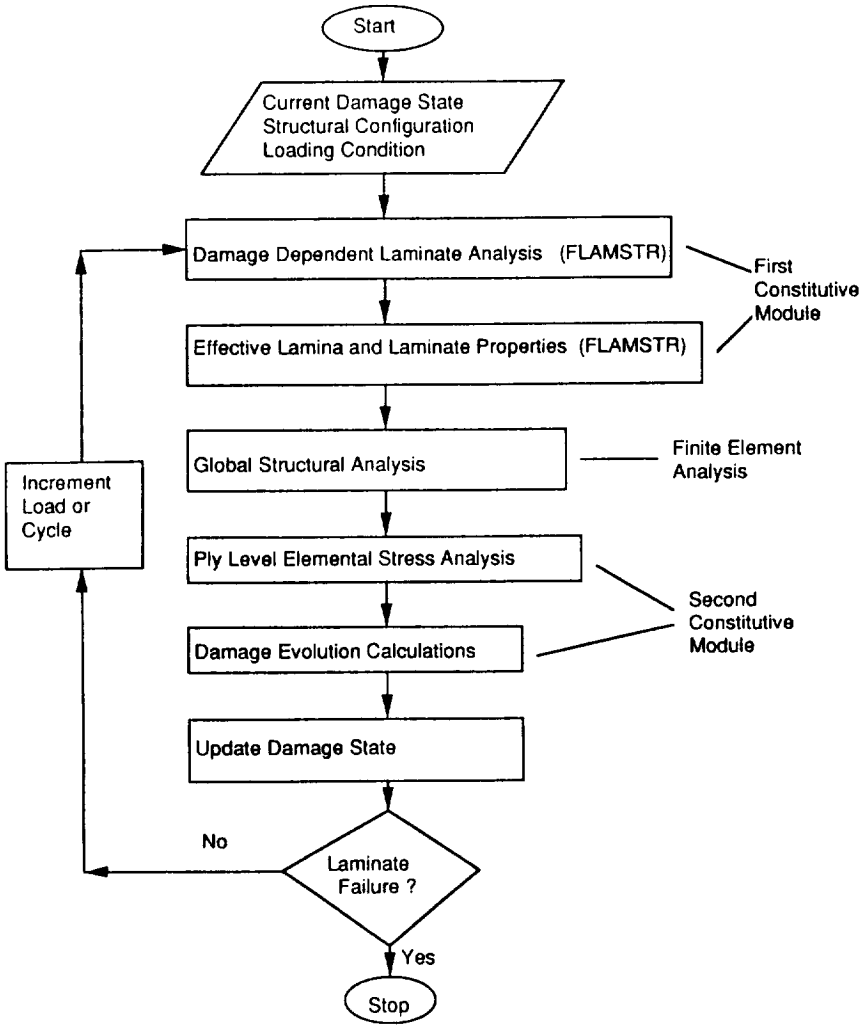

Figure 2. *Progressive failure analysis scheme.*

a description of the information needed as model input. A FORTRAN code consisting of the damage dependent constitutive model and a damage growth law for matrix cracking was incorporated into a classical lamination theory analysis to produce effective lamina and laminate properties for unnotched laminates. The program is called FLAMSTR (Fatigue LAMinate STRess) [19] and makes up the first constitutive module. The fourth block is a damage dependent finite element analysis code [18] from which the second constitutive module performs a ply level elemental stress analysis and simulates damage growth via damage growth laws for each element. Updating the damage state, block seven, for notched laminates is the result of the damage evolution calculations in block six. For unnotched laminates, only the first constitutive model is needed to update the damage state.

MATHEMATICAL FRAMEWORK FOR DAMAGE DEPENDENT LAMINATION MODEL

The damage model represents each mode of microcrack damage by the volume averaged dyadic product of the crack face displacement, u_i, and the crack face normal, n_j, as originally defined by Vakulenko and Kachanov [10],

$$\alpha_{ij} = \frac{1}{V_L} \int_{s_c} u_i^c n_j^c ds \tag{1}$$

where α_{ij} is the second order tensor internal state variable, s_c is the crack surface area, and V_L is the local representative volume, i.e., all stresses, strains, and ISVs are averaged over a local volume element. This product can be interpreted as additional strains incurred by the material as a result of the internal damage. The local ply level damage-dependent stress-strain relationship is given by [12],

$$\sigma_{ij_L} = \bar{Q}_{ijkl}\{\epsilon_{kl} - \alpha_{kl}\}_L \tag{2}$$

where σ_{ij_L} are the locally averaged components of stress, $\bar{Q}_{ijkl}$ is the ply level transformed stiffness matrix, ϵ_{kl_L} are the locally averaged components of strain, and α_{kl_L} are the components of the internal state variable. From here on out, the locally averaged subscript, L, will be dropped and all quantities are considered locally averaged unless specified otherwise. This ply level stress-strain relationship can be implemented directly into lamination theory. The laminate equations are constructed by assuming that the Kirchoff-Love hypothesis may be modified to include the effects of jump displacements u_i^D, v_i^D, and w_i^D as well as jump rotations β_i^D and ψ_i^D for the ith delaminated interface. Therefore, the displacement field in the x, y, and z directions is defined as [12]

$$\begin{aligned} u(x,y,z) &= u^o(x,y) - z[\beta^o + H(z - z_i)\beta_i^D] + H(z - z_i)u_i^D \\ v(x,y,z) &= v^o(x,y) - z[\psi^o + H(z - z_i)\psi_i^D] + H(z - z_i)v_i^D \\ w(x,y,z) &= w^o(x,y) + H(z - z_i)w_i^D \end{aligned} \tag{3}$$

where the superscripts o imply undamaged midsurface quantities, and $H(z - z_i)$ is the Heavyside step function. Locally averaging the displacement field provides the means to obtain the locally averaged components of strain as [12,20]

$$\begin{aligned}
\epsilon_x &= \frac{\partial u}{\partial x} \\
\epsilon_y &= \frac{\partial v}{\partial y} \\
\epsilon_z &= \frac{\partial w}{\partial z} \\
\epsilon_{yz} &= \frac{1}{2}\left\{\frac{\partial v}{\partial z} + \frac{\partial w}{\partial y}\right\} \\
\epsilon_{xz} &= \frac{1}{2}\left\{\frac{\partial u}{\partial z} + \frac{\partial w}{\partial x}\right\} \\
\epsilon_{xy} &= \frac{1}{2}\left\{\frac{\partial u}{\partial y} + \frac{\partial v}{\partial x}\right\}
\end{aligned} \tag{4}$$

which can be substituted back into the ply level damage-dependent stress-strain relationship [Equation (2)]. The laminate midplane forces and moments per unit width of region V_L in the laminate are given by [20]

$$\begin{aligned}
\begin{Bmatrix} N_x \\ N_y \\ N_{xy} \end{Bmatrix} &= \int_{-t/2}^{t/2} \begin{Bmatrix} \sigma_x \\ \sigma_y \\ \sigma_z \end{Bmatrix} dz \\
\begin{Bmatrix} M_x \\ M_y \\ M_{xy} \end{Bmatrix} &= \int_{-t/2}^{t/2} \begin{Bmatrix} \sigma_x \\ \sigma_y \\ \sigma_z \end{Bmatrix} z\,dz
\end{aligned} \tag{5}$$

Therefore, the resulting laminate equations are [12]

$$\{N\} = \sum_{k=1}^{n} [\bar{Q}]_k (z_k - z_{k-1})\{\epsilon^o\} - \frac{1}{2}\sum_{k=1}^{n} [\bar{Q}]_k (z_k^2 - z_{k-1}^2)\{\kappa\} + \sum_{i=1}^{d} [\bar{Q}_i^*]_i t_i \begin{Bmatrix} 0 \\ 0 \\ \alpha_{1i}^D \\ \alpha_{2i}^D \\ \alpha_{3i}^D \\ 0 \end{Bmatrix}$$

$$+\sum_{i=1}^{d}[\bar{Q}_i^*](z_i - z_{i-1})\begin{Bmatrix}0\\0\\0\\\alpha_{4i}^D\\\alpha_{5i}^D\\0\end{Bmatrix} - \sum_{k=1}^{n}[\bar{Q}]_k(z_k - z_{k-1})\{\alpha^M\}_k \tag{6}$$

$$\{M\} = \frac{1}{2}\sum_{k=1}^{n}[\bar{Q}]_k(z_k^2 - z_{k-1}^2)\{\epsilon^o\} - \frac{1}{3}\sum_{k=1}^{n}[\bar{Q}]_k(z_k^3 - z_{k-1}^3)\{\kappa\}$$

$$+\sum_{i=1}^{d}[\bar{Q}_i^*]_i t_i^2\begin{Bmatrix}0\\0\\\alpha_{1i}^D\\\alpha_{2i}^D\\\alpha_{3i}^D\\0\end{Bmatrix} + \sum_{i=1}^{d}[\bar{Q}_i^*](z_k^2 - z_{k-1}^2)\begin{Bmatrix}0\\0\\0\\\alpha_{4i}^D\\\alpha_{5i}^D\\0\end{Bmatrix}$$

$$-\frac{1}{2}\sum_{k=1}^{n}[\bar{Q}]_k(z_k^2 - z_{k-1}^2)\{\alpha^M\}_k \tag{7}$$

where $[\bar{Q}]_k$ is the undamaged transformed modulus of the kth ply in the laminate, z_k is the z-coordinate of the kth ply interface, ϵ^o are the locally averaged midsurface strains, and κ are the locally averaged midsurface rotations. Finally, $[\bar{Q}_i^*]$ are the averaged transformed stiffness matrices related to the ith delaminated ply interface, and the superscripts D and M represent delamination and matrix cracking, respectively.

From Equation (1), there are nine components of the internal state variable for any mode of damage. However, most of these components are zero. For intraply matrix cracks the resulting non-zero damage variables are α_{22}^M, α_{12}^M, and α_{32}^M. Since each ply has in-plane symmetry, α_{32}^M is negligible compared to the other components [12,21]. Delamination internal state variables are also defined by volume averaged displacements. Interface displacements, u_i^D, v_i^D, and w_i^D at the ith delamination sites are represented by α_{3i}^D, α_{2i}^D, and α_{1i}^D, respectively. Delamination induced rotations about the x and y axes, ψ_i^D and β_i^D, are represented by α_{4i}^D and α_{5i}^D, respectively. All other components are zero [12,21].

Mode I Matrix Crack Growth Law

A damage growth law has been developed for mode I matrix cracks, α_{22}^M, where the displacement of the crack face is in a direction parallel to the crack face normal, i.e., perpendicular to the plane formed by the ply. The mode I strain energy release rate is calculated from the following equation [19,21],

$$G_1 = V_L C_{ij22}(\epsilon_{ij} - \alpha_{ij}^M)\frac{\partial \alpha_{22}^M}{\partial s} \tag{8}$$

where $\partial\alpha_{22}^{M}/\partial s$ is a linear function of the local ply stresses and describes the change in the internal state variable for a certain change in crack surface area, and can be written as

$$\frac{\partial\alpha_{22}^{M}}{\partial s} = (d\text{para})(\sigma_{22}) \tag{9}$$

where $d$para is a material dependent parameter [19] which must be determined experimentally. Therefore, the damage growth law for uniaxial cyclic loading is given by [16,19]

$$\frac{\partial\alpha_{22}^{M}}{\partial N} = \frac{\partial\alpha_{22}^{M}}{\partial s} kG_{I}^{\eta} \tag{10}$$

where k and η are experimentally determined material dependent parameters, N is the number of load cycles, and G_I is the mode I strain energy release rate for the ply of interest.

Mode I Delamination Empirical Formulation

The following relationship [12] provides an empirical formula with which to calculate the internal state variable due to delamination

$$\frac{\partial\alpha_{3}^{D}}{\partial\epsilon_{x}} = -\frac{n}{2}\frac{(E_{xo} - E^{*})}{\bar{Q}_{11}^{T} + \bar{Q}_{11}^{B}}\left(\frac{S_D}{S}\right) \tag{11}$$

where E_{xo} is the undamaged experimental stiffness and E^* is the moduli of the sublaminates formed by delamination [22,23]. Furthermore, n is the total number of plies, S_D is the delamination surface area, S is the total surface area, and $\bar{Q}_{11}^{T}$ and $\bar{Q}_{11}^{B}$ are the transformed stiffnesses of the plies above and below the delamination formed by regions of delamination at the midplane.

MODELS FOR DAMAGE GROWTH

The material IM7/5260 was chosen to experimentally verify the continuum damage model. Unlike the brittle material, AS4/3502 used to develop the model, IM7/5260 has a toughened resin, and it was thought that this material would test the applicability of the model to a toughened matrix composite. The experimental procedure was designed based upon the data needed to successfully use the model.

Three material parameters, $d$para, k, and η, must be determined experimentally. The calculations involved in determining the model parameters have been previously published in detail [19,24]. The material parameters can be shown to be determined from the mode I internal state variable, α_{22}^{M}. This was accomplished by subjecting $[0/90_2/0]_s$ laminates to tension-tension fatigue [24] with maximum stress levels at 30% ultimate stress. Edge replicas and X-rays were

used to measure crack surface area and determine crack density in the 90 degree plies. The ply level transverse and shear moduli were determined from unidirectional and $[45/-45]_2$, laminates [25]. The internal state variable, α_{22}, was calculated for each crack density measurement utilizing the following equations [15,19]

$$\alpha_{22} = \frac{\frac{\varrho}{2\bar{t}}}{\frac{\pi^4}{64\xi} - C_{2222}} \tag{12}$$

$$\xi = \sum_m \sum_n \frac{1}{C_{2222}(2m-1)^2(2n-1)^2 + C_{1212}\left(\frac{\bar{a}}{\bar{t}}\right)^2(2n-1)^4} \tag{13}$$

where ϱ is the force per unit length applied transverse to the 90 degree fibers, $2\bar{t}$ and $1/2\bar{a}$ are the layer thickness and crack density, respectively, and $\varrho/2\bar{t}$ is basically the local stress (σ_2) in the 90 degree plies. C_{2222} is the transverse modulus, C_{1212} is the shear modulus, and m and n are the number of iterations. Furthermore, $d\alpha_{22}/ds$ is obtained by plotting α_{22} as a function of crack surface area (Figure 3). This results in the following equations [24]

$$\alpha_{22} = -1.57 \times 10^{-6} + (2.91 \times 10^{-4})(s) + (1.22 \times 10^{-5})(s^2) \tag{14}$$

$$\frac{d\alpha_{22}}{ds} = 2.91 \times 10^{-4} + (2.45 \times 10^{-5})(s) \tag{15}$$

where s is the crack surface area. Referring to Equation (9), the first material parameter, $d$para, was found as the slope of $d\alpha_{22}/ds$ vs. the local stress in the 90 degree plies, σ_2.

Plotting α_{22} as a function of the number of cycles (Figure 4) resulted in the following equations [24]

$$\alpha_{22} = -4.81 \times 10^{-6} + (3.49 \times 10^{-9})N - (4.77 \times 10^{-5})N^2 \tag{16}$$

$$\frac{d\alpha_{22}}{dN} = 3.49 \times 10^{-9} - (9.54 \times 10^{-15})N \tag{17}$$

Furthermore, the mode I ply level strain energy release rate, G, could be calculated as

$$G_1 = (t)\left(\frac{d\alpha_{22}}{ds}\right)(\sigma_2) \tag{18}$$

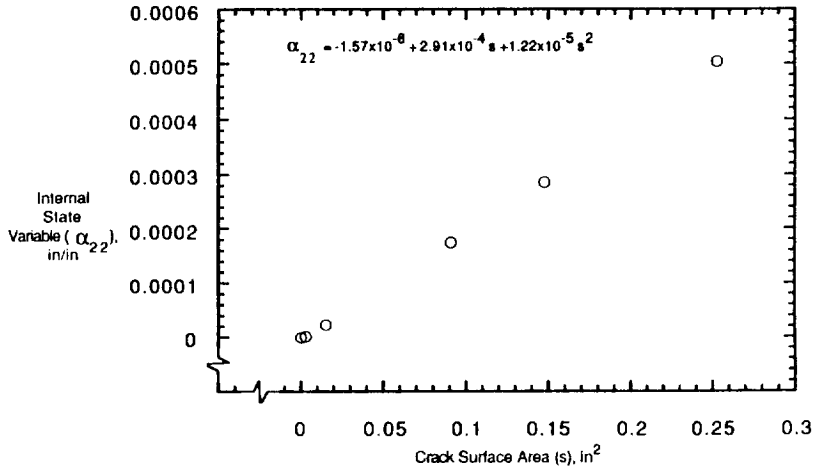

Figure 3. *Internal state variable for matrix cracks in IM7/5260 as a function of crack surface area.*

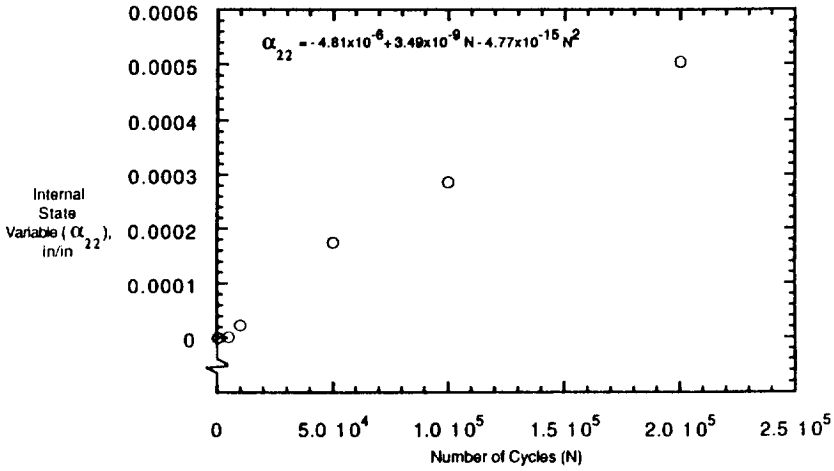

Figure 4. *Internal state variable for matrix cracks in IM7/5260 as a function of fatigue cycles.*

since $d\alpha_{22}/ds$ and σ_2 are known over the given number of cycles. The ply thickness, t, is actually the thickness of the consecutive ninety degree plies, i.e., t is equal to two times the thickness of one ply for a $[0/90_2/0]_s$ laminate, whereas t is equal to the thickness of one ply in a [0/90/0], laminate. Finally, rearranging the damage growth law [Equation (10)] to the form

$$\frac{ds}{dN} = \frac{d\alpha_{22}/dN}{d\alpha_{22}/ds} = kG_I^{\eta} \tag{19}$$

from Equations (15) and (17) $(d\alpha_{22}/dN)/(d\alpha_{22}/ds)$ was plotted as a function of the mode I strain energy release rate, G_I. A power curve was fit to the plotted data and, as a result, the final material parameters, k and η were obtained. The parameters were then used in a fatigue laminate stress program (FLAMSTR) [19] utilizing the damage-dependent lamination theory to predict reductions in stiffness due only to mode I matrix cracking for unnotched composite laminates.

Other contributors to stiffness loss are delamination damage and matrix cracking due to shear. The following general equation can be used to predict reductions in stiffness for any laminate [21]

$$\frac{E_x}{E_{xo}} = 1 - \frac{\Delta E^M}{E_{xo}} - \frac{\Delta E^D}{E_{xo}} - \frac{\Delta E^S}{E_{xo}} \tag{20}$$

where ΔE^M, ΔE^D, and ΔE^S refer to the change in stiffness due to mode I matrix cracking, delamination, and matrix cracking in the 45 degree plies, respectively. However, we assume the stiffness loss due to the 45 degree ply matrix cracks is negligible and therefore ignore it primarily because previous work [24] showed the effects of these 45 degree ply cracks to be small compared to other modes of damage. Furthermore, based on results from a separate study [26], plastic strain in these laminates was negligible at the applied stress levels. Delamination, on the other hand has a dominant effect. We define $\Delta E^D/E_{xo}$ by the following equation for any number of delamination sites as [21]

$$\frac{\Delta E_x^D}{E_{xo}} = \frac{1}{TE_{xo}} \sum_{i=1}^{d} [\bar{Q}_{1s}]_i t_i \left\{ \frac{\partial \alpha_{3i}^D}{\partial \epsilon_x} \right\} \tag{21}$$

where

$$\bar{Q}_{1s} = \frac{\bar{Q}_{11}^T + \bar{Q}_{11}^B}{2} \tag{22}$$

which, by substituting Equation (11) into Equation (21), can be reduced to

$$\frac{\Delta E^D}{E_{xo}} = \left(1 - \frac{E^*}{E_{xo}}\right)\left(\frac{S_D}{S}\right) \tag{23}$$

The use of Equation (23), which is identical to O'Brien's equation for stiffness of a partially delaminated laminate [22], requires the experimental determination of the delamination area S_D. As such, the model is only correlative for delamination damage. Furthermore, the computation of E^* must be made on the basis of whether the delamination is an edge delamination versus a local delamination that initiates at a matrix crack [27].

MATERIALS AND EXPERIMENTAL PROCEDURE

As previously mentioned, the material chosen to experimentally verify the continuum damage model was IM7/5260 graphite/bismaleimide laminates. Cross-ply and quasi-isotropic laminates were cut into 2.54 cm × 25.4 cm (1″ × 10″) coupons. The layups used were $[0/90_2/0]_s$, $[0/90_3]_s$, $[0/45/-45/90]_s$, and $[90/-45/45/0]$, notched and unnotched. The notched laminates had a 6.35 mm (1/4 inch) hole drilled in the center. Each laminate was subjected to tension-tension fatigue up to 100,000 cycles at a frequency of 5 Hz and a stress ratio of 0.1. Six specimens of each layup were fatigued such that three specimens were fatigued at maximum load levels of 30% of ultimate failure load and three more at 65%. In situ edge replicas and X-ray radiographs to characterize damage were taken throughout the testing so that the specimen did not have to be removed from the load frame. A Direct Current Displacement Transducer (DCDT) with a 4″ gage length was secured to the specimen and remained secured and untouched for the entire test. The fatigue loading was stopped periodically to collect edge replicas and X-rays, and to monotonically load the specimen for strain measurements.

EXPERIMENTAL CHARACTERIZATION

To experimentally verify the model, experimental stiffness loss directly correlating to damage accumulation was compared to model predictions. The following procedure was used to document stiffness loss and characterize damage. The function of the DCDT was to measure increases in strain due to damage accumulation over a 4″ gage length. Initial strain measurements as well as edge replicas and X-rays were taken to ensure no initial damage and establish the initial undamaged stiffness. Periodic strain measurements, edge replicas, and X-rays showed a degrading trend in stiffness with damage accumulation. The in situ edge replicas and X-ray radiographs provided a direct and accurate correlation between damage accumulation and stiffness loss. The edge replicas and X-ray radiographs provided the means to measure matrix crack and delamination surface areas. At the end of the test, the specimens were monotonically loaded to failure. Comparing these failure loads with the failure loads of the undamaged specimens provides the residual strength at 100,000 cycles for a given fatigue stress level.

EXPERIMENTAL VERIFICATION OF MODEL

The material parameters, $d$para, k, and η, are determined from the mode I matrix crack surface area. The unnotched $[0/90_2/0]_s$ laminates provided this in-

formation since the matrix cracks in the 90 degree plies are strictly mode I and no cracks accumulate in the 0 degree plies. The crack surface area as a function of fatigue cycles was measured from the edge replicas and the X-ray radiographs [24]. From there, the matrix crack internal state variables were calculated and used to determine the material parameters as mentioned previously in the section "Models for Damage Growth." The parameters are then used in the mode I matrix crack growth law to compare stiffness loss predictions due only to mode I matrix cracking to the experimental stiffness loss of the other notched and unnotched laminates. For those laminates with delaminations, the stiffness degradation was greater. The delamination surface area and delamination locations, as determined from the X-ray radiographs and the edge replicas, respectively, were used in conjunction with Equation (24) to provide a prediction of stiffness loss due to delamination.

RESULTS

The analysis of the experimental data provided the following material parameters:

$$d\text{para} = 8.8686 \times 10^{-7}/\text{lb}$$

$$k = 1.1695 \frac{\text{in}^2}{\text{cycle}\left(\frac{\text{in-lb}}{\text{in}^2}\right)^{\eta}}$$

$$\eta = 5.5109$$

These parameters were then used, via the mode I matrix cracking growth law, in a fatigue laminate stress program (FLAMSTR) [19] and a damage dependent finite element code installed in the COMET [18] to predict reductions in stiffness due only to mode I matrix cracking illustrated in Figure 5 for $[0/90_3]_s$ laminates. These predictions are illustrated in Figure 6 where we see that the predicted reductions in stiffness are in close agreement with the experimental stiffness loss due solely to mode I matrix cracking in the 90 degree plies of the $[0/90_3]_s$ laminates. Not only are these two distinct trends predicted from two different constant amplitude maximum stress levels, but the predicted trends follow the experimental data very well. The X-ray radiographs in Figure 5 exactly correlate with one data point in Figure 6 for each constant amplitude maximum stress level, and two separate trends in stiffness loss were observed for two separate damage states.

If delamination is also considered, damage-dependent empirical formulas may be used to determine the predicted reductions in stiffness due to delamination. The $[0/45/-45/90]_s$ laminates suffered edge delamination primarily at the $-45/90$ interface. A comparison of the delamination surface area with measured stiffness loss at 100,000 cycles is illustrated in Figure 7. The experimentally measured delamination surface areas were used in Equation (24) to predict stiffness loss due to delamination growth. The experimental results with their

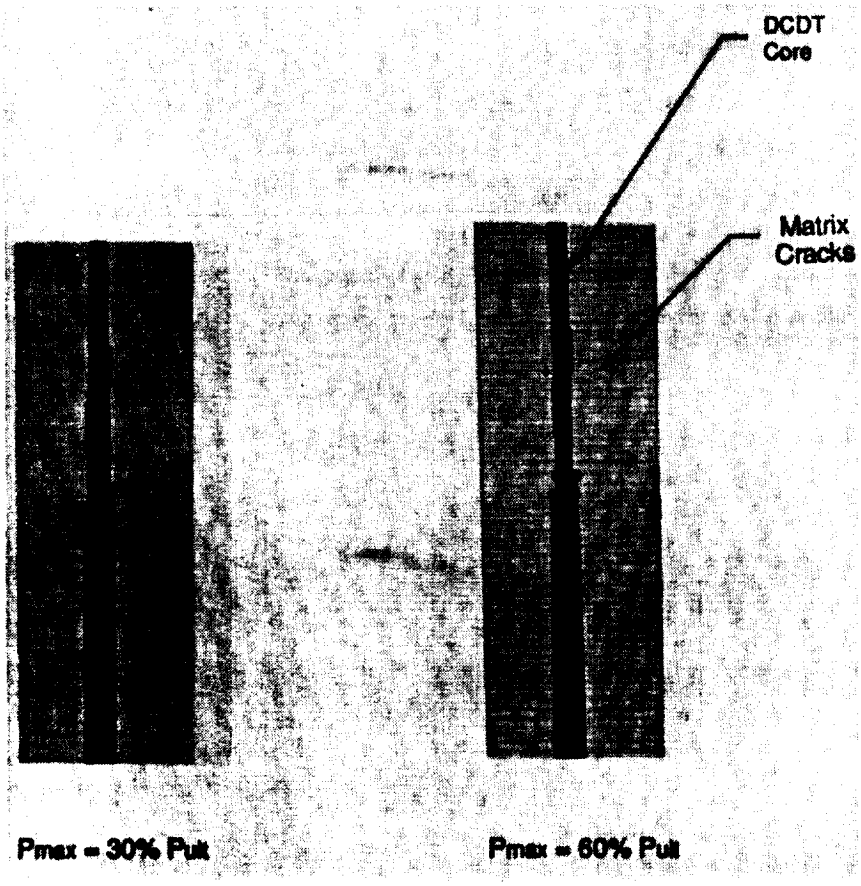

Figure 5. Loading history effect on mode I matrix cracking in $[0/90_3]_s$ IM7/5260 at 100,000 cycles.

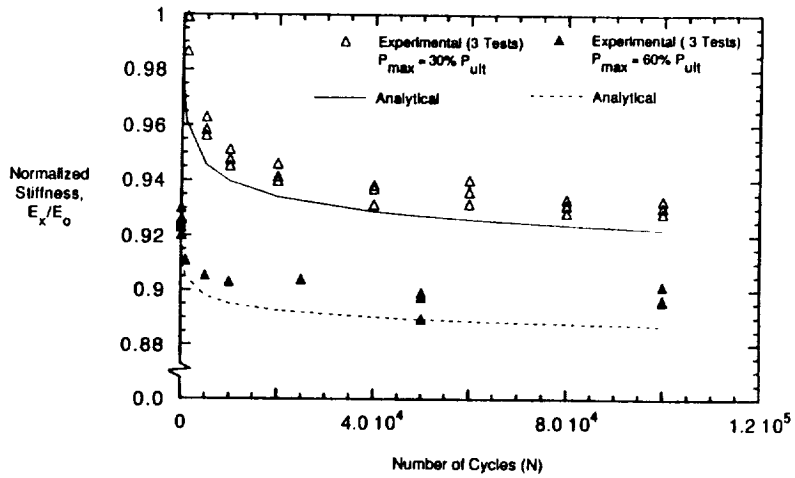

Figure 6. *Experimental vs. analytical stiffness degradation of* $[0/90_3]_s$ *IM7/5260 for tension-tension fatigue.*

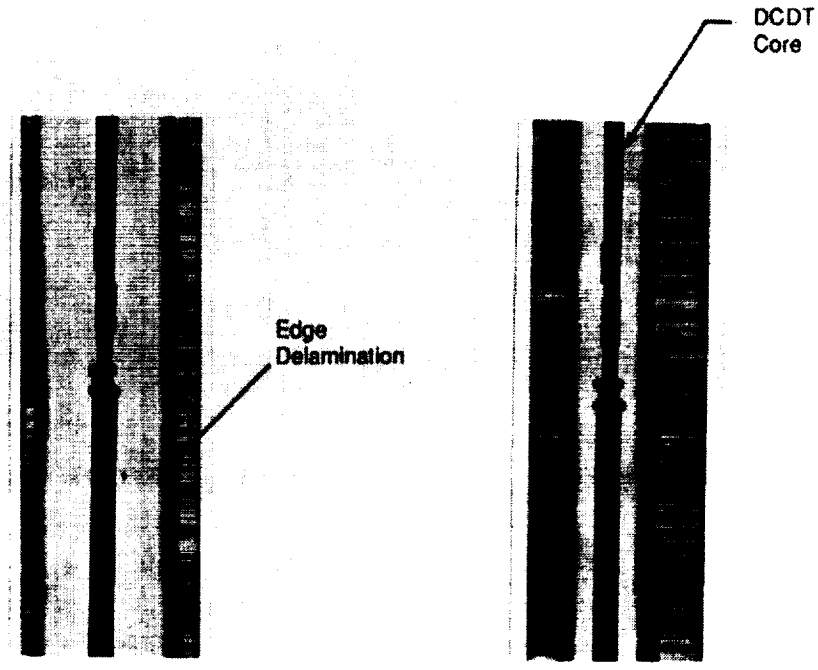

Figure 7. *X-ray radiograph of* $[0/45/-45/90]_s$ *IM7/5260 at 100,000 cycles.*

predictions for laminates subjected to 50% and 60% of ultimate load are shown in Figures 8 and 9. A graphical comparison of these two loading histories is shown in Figure 10. Once again, the model predicted greater stiffness loss for a greater maximum stress level. Furthermore, as was expected, stiffness loss in these laminates was not greatly affected by the mode I matrix cracking alone.

To further verify the delamination empirical formula for stiffness loss, Equation (24) was applied to a different stacking sequence. A comparison of the different stacking sequence is illustrated in Figure 11 where the arrows indicate locations of primary local and edge delaminations for the $[90/-45/45/0]_s$ and $[0/45/-45/90]_s$ layups, respectively. The X-ray radiographs in Figure 11 show a distinct difference in the damage state and a larger reduction in stiffness per delamination surface area for the $[90/-45/45/0]_s$ laminate. Figure 12 is the experimental and predicted stiffness loss of a $[90/-45/45/0]_s$ laminate. Close attention should be paid here to the difference between E^* for edge delamination vs. local delamination [27].

The analysis of the notched laminates yielded good results as well. An illustration of the damage commonly seen in a notched laminate for two different stacking sequences is shown in Figure 13. Initially, one would expect the matrix crack in the zero degree ply adjacent to the hole (axial split) to have a significant effect in reducing the stress concentration at the notch. This would increase the global displacements of the laminate prior to failure. A damage dependent finite element code [18] within the NASA COMET was used to calculate mode I matrix cracking damage variables, laminate stresses and strains, and far field displacements. The finite element mesh in Figure 14 is a quarter section of the notched laminate. The finite element code predicts the damage state in each element as a function

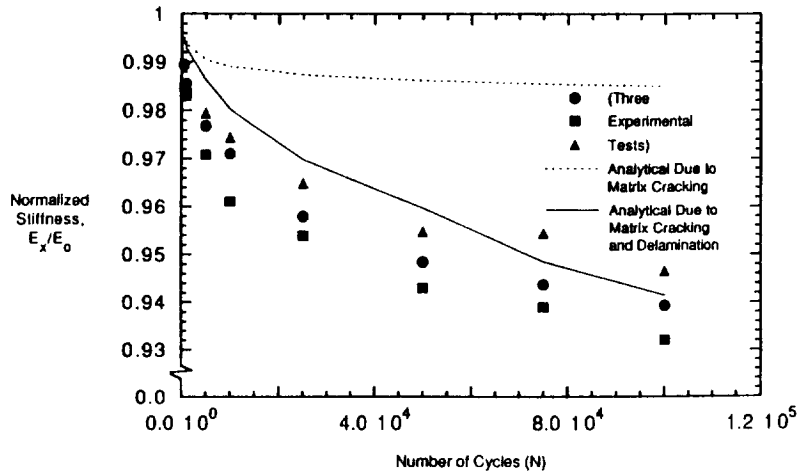

Figure 8. *Experimental vs. analytical stiffness degradation of $[0/45/-45/90]_s$ IM7/5260 for tension-tension fatigue at P_{max} = 50% Pult.*

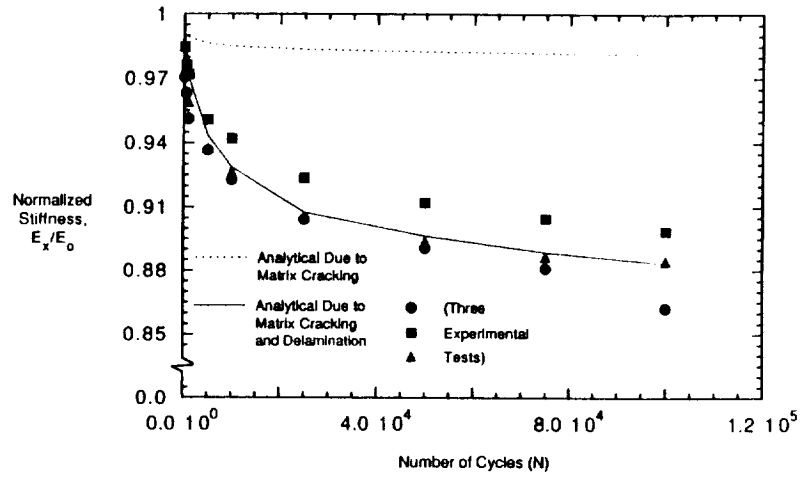

Figure 9. *Experimental vs. analytical stiffness degradation of [0/45/ – 45/90]$_s$ IM7/5260 for tension-tension fatigue at P_{max} = 60% Pult.*

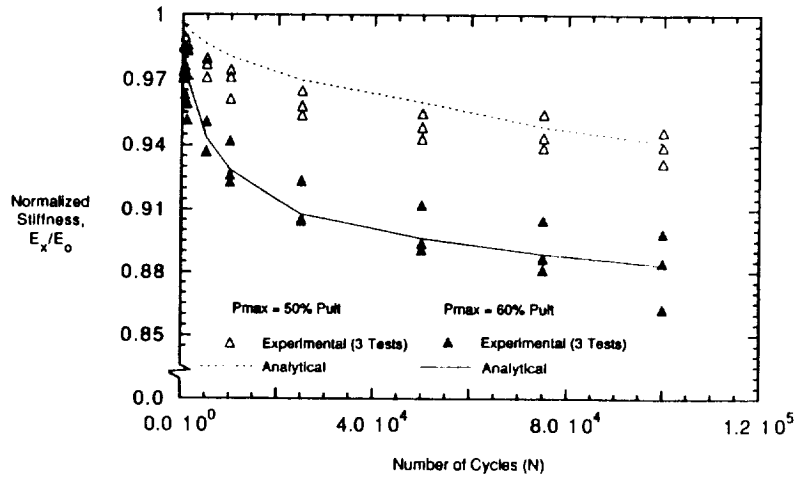

Figure 10. *Experimental vs. analytical stiffness degradation of [0/45/ – 45/90]$_s$ IM7/5260 for tension-tension fatigue.*

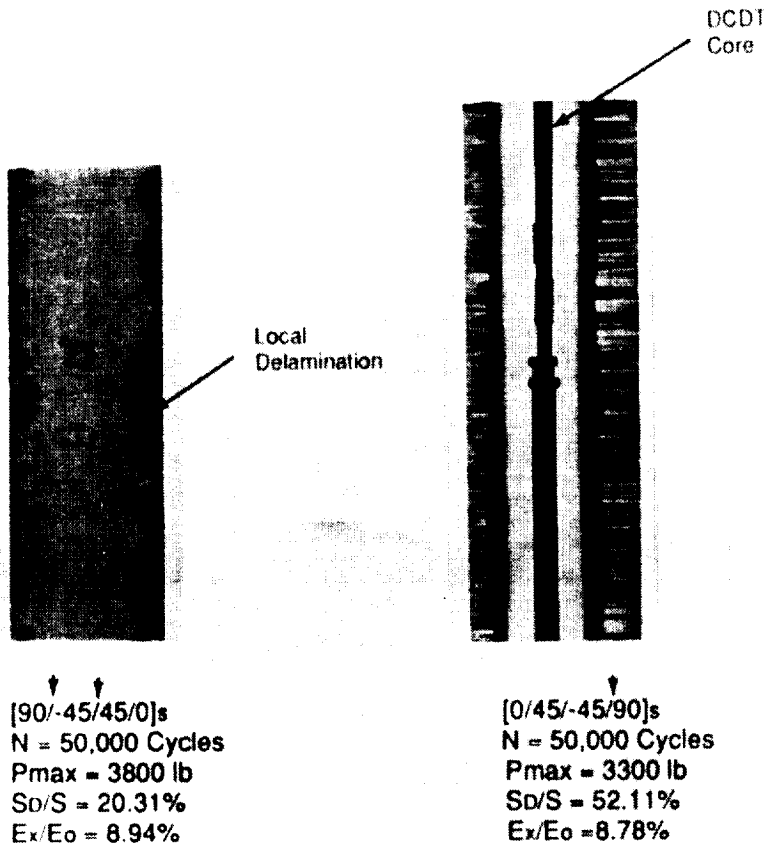

Figure 11. *X-ray radiograph of quasi-isotropic IM7/5260 laminates.*

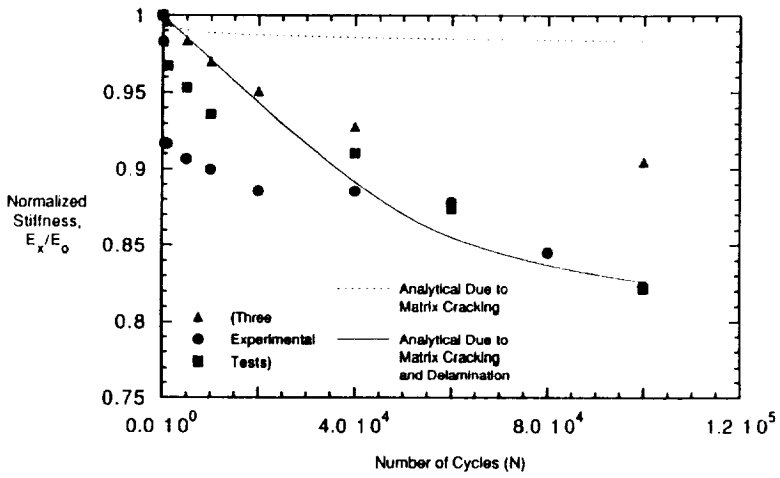

Figure 12. *Stiffness degradation of* $[90/-45/45/0]_s$ *IM7/5260.*

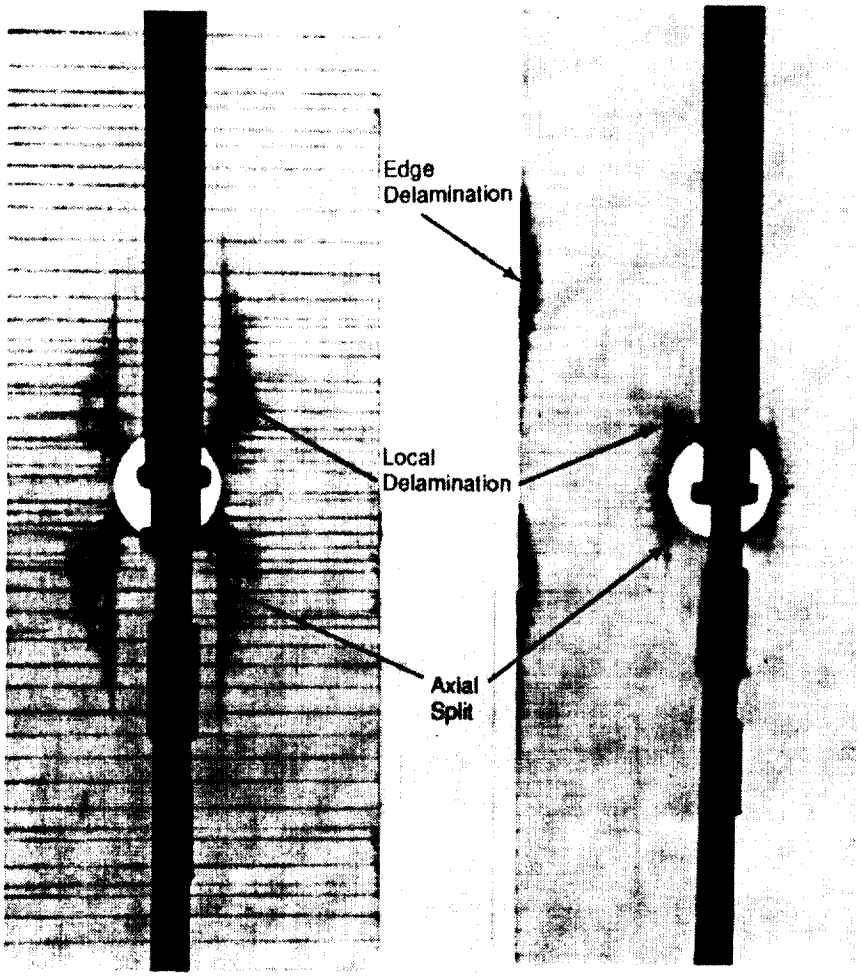

Figure 13. X-ray radiograph of IM7/5260 notched laminates.

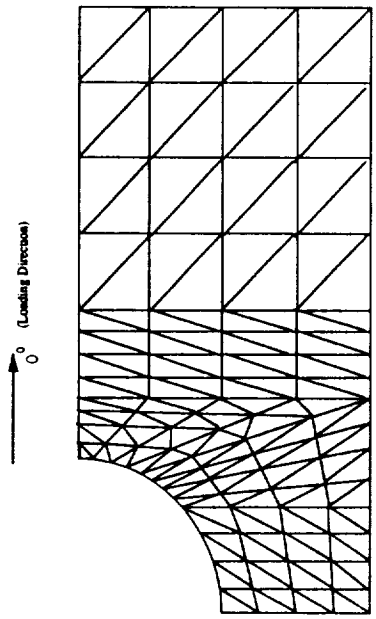

Figure 14. *Finite element mesh for laminates with a central circular notch.*

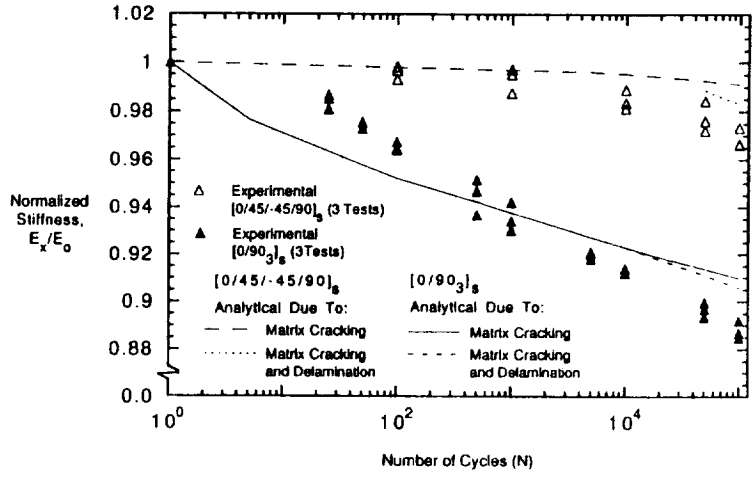

Figure 15. *Stiffness loss of IM7/5260 laminates with a central circular notch.*

of the local element stresses. An iterative procedure is used to calculate the element damage-dependent properties and associated load redistribution throughout the finite element model. The analytical far field displacements calculated over a 4″ gage length are compared to the experimental stiffness loss in Figure 15. This figure illustrates the ability of the code to predict separate trends in stiffness reductions due to mode I matrix cracking for different constant amplitude stress levels and layups for a spatially varying damage state. Edge and local delaminations were also figured into the predictions and were found to have very little effect, especially compared to the mode I matrix cracking of the axial split for the $[0/90_3]_s$ laminate. This is attributed to the small delamination surface areas as well as the fact that the difference between E^* and E_{xo} is small. The comparison of the two laminates given in Figures 13 and 15 confirms the ability of this model to predict damage growth as a function of the laminate stacking sequence. The $[0/90_3]_s$ laminate has more severe axial splitting, i.e., more mode I matrix cracking, thus the predicted loss in stiffness due to mode I matrix cracking is larger. The reductions in stiffness are greater for this laminate because more load is transferred away from the stress concentration at the hole.

CONCLUSIONS

The damage model originally developed by Allen and Harris was applied to the IM7/5260 toughened matrix material system. Experimental verification of the model was established by comparing the stiffness loss of cross-ply and quasi-isotropic laminates with and without open holes for tension fatigue loadings. The model has predictive capability for intraply matrix cracks and correlative capability for delaminations. The model successfully predicted both the effects of laminate stacking sequence and loading history on damage growth and stiffness loss. The ability of the model to predict damage growth in the open hole specimens was particularly encouraging. This illustrates that the model is appropriate for spatially varying damage and not confined to uniform damage that typically develops in the gage length of an unnotched uniaxial test specimen. The spatial variation in damage is treated through the finite element discretization since the damage is assumed to be uniform within an element. The empirical formulae for delamination provided trends in stiffness loss that agreed with the experimental trends. It should be noted here, however, the predictive capability of this model would increase dramatically if delamination growth laws were available rather than the empirical relations which need the extent of the delamination to be specified rather than predicted.

NOMENCLATURE

$\bar{a}$	two times crack density
C_{ijkl}	ply level stiffness tensor
$d$para	material parameter—slope of $d\alpha/ds$ vs. local ply stress
E^*	axial stiffness of a laminate completely delaminated along one or more interfaces

E_{xo} undamaged longitudinal stiffness
E_x/E_{xo} longitudinal stiffness loss
G_I mode I strain energy release rate
$(G_{12})_{exp}$ experimental shear modulus at final cycle
G_{12o} undamaged shear modulus
k growth law material parameter
n number of plies
n_i^c crack face normal
$[\bar{Q}]$ ply level transformed stiffness matrix
$\bar{Q}_1, \bar{Q}_2, \bar{Q}_3, \bar{Q}_4$ average transformed stiffness matrices of sublaminates formed by delaminations
$\bar{Q}_{11}^t$ stiffness at the top sublaminate at a delamination interface
$\bar{Q}_{11}^B$ stiffness of the bottom sublaminate at a delamination interface
s_c crack surface area
S_D delamination surface area
S total surface area
$\bar{t}$ one-half ply thickness
t thickness of consecutive 90 degree plies
T laminate thickness
t_i twice the ply thickness
u_i^c crack face displacement
u, v, w locally averaged displacements
$u^o(x, y), v^o(x, y), w^o(x, y)$ undamaged midsurface displacements
u_i^D, v_i^D, w_i^D delamination interface displacements
V_L local representative volume
z_k z coordinate of the kth ply interface
α_{ij}^M matrix cracking internal state variable
α_{kl}^D delamination internal state variable
β_i^D, ψ_i^D delamination induced rotations
$\Delta E^M/E_{xo}$ mode I matrix cracking stiffness reductions
$\Delta E^S/E_{xo}$ 45 degree ply matrix cracking stiffness reductions
$\Delta E^D/E_{xo}$ delamination stiffness reductions
ϵ locally averaged components of strain
$\varkappa$ locally averaged midsurface rotations
η growth law material parameter
ϱ force per unit length applied transverse to the 90 degree plies
σ locally averaged components of stress
σ_2 local stress in the 90 degree plies

REFERENCES

1. Reifsnider, K. L. 1980. "Fatigue Behavior of Composite Materials," *International Journal of Fracture*, 16(6):563–583.

2. Reifsnider, K. L. 1981. "The Mechanics of Fatigue in Composite Laminates," in *Composite Materials*, K. Kawata and T. Adasada, eds., *Proc. Japan-U.S. Conference*, Tokyo, pp. 131–144.

3. Talug, A. and K. L. Reifsnider. 1979. "Analysis of Stress Fields in Composite Laminates with Interior Cracks," *Fiber Science and Technology*, 12:201–215.

4. O'Brien, T. K. 1990. "Towards a Damage Tolerance Philosophy for Composite Materials and Structures," in *Composite Materials: Testing and Design (Ninth Volume), ASTM STP 1059*, S. P. Garbo, ed., Philadelphia: American Society for Testing and Materials, pp. 7–33.

5. Chang, F.-K. and K.-Y. Chang. 1987. "A Progressive Damage Model for Laminated Composites Containing Stress Concentrations," *J. of Composite Materials*, 21:834–855.

6. Chamis, C. C., P. L. N. Murphy and L. Minnetyan. 1992. "Structural Behavior of Composites with Progressive Fracture," *J. of Reinforced Plastics and Composites*, 11:413–442.

7. Talreja, R. 1985. "A Continuum Mechanics Characterization of Damage in Composite Materials," *Proc. R. Soc. London*, 399A:126–216.

8. Talreja, R. 1985. "Residual Stiffness Properties of Cracked Composite Laminates," *Advances in Fracture Research, Proc. Sixth Int. Conf. De Fracture*, New Delhi, India, 4:3013–3019.

9. Talreja, R. 1985. "Transverse Cracking and Stiffness Reduction in Composite Laminates," *J. of Composite Materials*, 19:355–375.

10. Vakulenko, A. A. and M. L. Kachanov. 1971. "Continuum Theory of Cracked Media," *Izv. AN SSR. Mekhaniha Tverdogo Tela*, 6:159.

11. Harris, C. E., D. H. Allen and T. K. O'Brien. 1990. "Progressive Failure Methodologies for Predicting Residual Strength and Life of Laminated Composites," *Proceedings of 1st NASA Advanced Composites Technology Conference*, Oct. 30–Nov. 1.

12. Allen, D. H., S. E. Groves and C. E. Harris. 1988. "A Cumulative Damage Model for Continuous Fiber Composite Laminates with Matrix Cracking and Interply Delamination," in *Composite Materials: Testing and Design (8th Conference), ASTM STP 972*, J. D. Whitcomb, ed., Philadelphia: American Society for Testing and Materials, pp. 57–80.

13. Allen, D. H., C. E. Harris and S. E. Groves. 1987. "A Thermomechanical Constitutive Theory for Elastic Composites with Distributed Damage – I. Theoretical Development," *Int. J. Solids Structures*, 23(9):1301–1318.

14. Allen, D. H., C. E. Harris and S. E. Groves. 1987. "A Thermomechanical Constitutive Theory for Elastic Composites with Distributed Damage – II. Application to Matrix Cracking in Laminated Composites," *Int. J. Solids Structures*, 23(9):1319–1338.

15. Lee, J. W., D. H. Allen and C. E. Harris. 1989. "Internal State Variable Approach for Predicting Stiffness Reductions in Fibrous Laminated Composites with Matrix Cracks," *J. of Composite Materials*, 23:1273–1291.

16. Lo, D. C., D. H. Allen and C. E. Harris. 1990. "A Continuum Model for Damage Evolution in Laminated Composites," *IUTAM Symposium on Inelastic Deformation of Composite Materials*.

17. Harris, C. E. and D. H. Allen. 1988. "A Continuum Damage Model of Fatigue-Induced Damage in Laminated Composites," *SAMPE Journal* (July/August):43–51.

18. Lo, D. C., D. H. Allen and C. E. Harris. "A Procedure for the Performance of Progressive Failure Analysis on the Computational Structural Mechanics Testbed," NASA Technical Memorandum 109155, NASA LaRC.

19. Lo, D. C., D. H. Allen and C. E. Harris. 1992. "A Procedure for Utilization of a Damage-Dependent Constitutive Model for Laminated Composites," NASA Technical Memorandum 104219, NASA LaRC, February.

20. Jones, R. M. 1975. *Mechanics of Composite Materials*. Hemisphere Publishing Corporation.

21. Nottorf, E. W. 1990. "An Investigation into the Effects of Damage on the Stresses in a Composite Laminate," Ph.D. dissertation, Texas A&M, August.

22. O'Brien, T. K. 1982. "Characterization of Delamination Onset and Growth in a Composite Laminate," in *Damage in Composite Materials, ASTM STP 775*, K. L. Reifsnider, ed., American Society for Testing and Materials, pp. 140–167.

23. O'Brien, T. K. 1993. "Local Delamination in Laminates with Angle Ply Matrix Cracks, Part II: Delamination Fracture Analysis and Fatigue Characterization," in *Composite Materials: Fatigue and Fracture, Fourth Volume, ASTM STP 1156*, W. W. Stinchcomb and N. E. Ashbaugh, eds., Philadelphia: American Society for Testing and Materials, pp. 507–538.

24. Coats, T. W. 1992. "Experimental Verification of a Progressive Damage Model for Composite Laminates Utilizing Continuum Damage Mechanics," Master's thesis, Old Dominion University, December.

25. Gates, T. S. 1991. "Experimental Characterization of Non-Linear Rate Dependent Behavior in Advanced Polymer Matrix Composites," *Experimental Mechanics SEM Spring Conference*, Milwaukee, WI, June 1991.

26. Gates, T. S. 1993. "Effects of Elevated Temperature on the Viscoplastic Modeling of Graphite/Polymeric Composites," in *High Temperature and Environmental Effects on Polymeric Composites, ASTM STP 1174*, C. E. Harris and T. S. Gates, eds., Philadelphia: American Society for Testing and Materials, pp. 201–221.

27. O'Brien, T. K. 1985. "Analysis of Local Delamination and Their Influence on Composite Laminate Behavior," *Delamination and Debonding of Materials*, Philadelphia, pp. 282–297.